

# Low Turn-on Voltage and High Breakdown GaN Schottky Barrier Diodes for RF Energy Harvesting Applications

Chung-Hsin Li<sup>1</sup>, Haoran Wang<sup>1</sup>, Yeke Liu<sup>1</sup>, Sumin D. Joseph<sup>2</sup>, Yi Huang<sup>2</sup>, and Shawn S. H. Hsu<sup>1</sup>

<sup>1</sup> Institute of Electronics Engineering, NTHU, Hsinchu 30013, Taiwan

Phone : +886-3-5731278, E-mail : shhsu@ee.nthu.edu.tw

<sup>2</sup> Dept. of EEE, University of Liverpool, Liverpool L69 3GJ, United Kingdom

Phone : +44-151-794-4521, E-mail : Yi.Huang@liverpool.ac.uk

## Abstract

This work presents design, fabrication, and analysis of GaN Schottky barrier diodes with low turn-on voltage  $V_{on}$  and high breakdown voltage  $V_{BK}$  on the silicon substrate with various layout parameters, aiming for RF energy harvesting applications. The measured results demonstrate a low  $V_{on}$  and a high  $V_{BK}$  of 0.56 V and 47 V, respectively. A high cut-off frequency of 360.9 GHz under reverse bias of -10 V is also obtained for a two-finger device with each finger of  $W = 12.5 \mu\text{m}$  and  $L = 0.2 \mu\text{m}$ .

## 1. Introduction

The trend of Internet of Things (IoT) predicts to have over 50 billion devices to be connected in 2020, including many sensors for various applications. One major issue for these sensors is the power supply. Using batteries may not be a good solution since these sensors could be deployed in various locations and replacement of the batteries becomes very inefficient. RF energy harvesting provides an attractive solution, which can recycle the abundant EM energy from the wireless signals for the power supply of sensors [1]. The Schottky barrier diode (SBD) is an essential component for converting the RF energy to DC power [2]. The diodes with low turn-on voltage and low on resistance ( $R_{ON}$ ) are important which can enhance the conversion efficiency. Also, a high breakdown voltage of the diode is preferred to improve the system robustness since a very high EM energy could be encountered in some occasions.

As a wide bandgap material, GaN has a very high breakdown field and an extremely high saturation electron velocity. As a result, the GaN-based SBD is an excellent candidate for RF energy harvesting applications. Recent progress also reported high-quality GaN epi layers grown on large-scale silicon substrates, making low cost and high performance GaN SBDs possible [3, 4]. In this paper, we demonstrate high frequency multi-finger AlGaN/GaN SBDs on the silicon substrate. Devices with different layout geometries are designed, fabricated, and investigated for both DC and RF characteristics. In addition, small-signal model parameters are extracted from the measured S-parameters for details analysis.

## 2. Device Structure and Fabrication

The epitaxial layers consist of 100-nm AlN initial buffer layer, 4.3- $\mu\text{m}$  carbon-doped GaN buffer, 500-nm GaN channel layer, 25-nm  $\text{Al}_{0.25}\text{Ga}_{0.75}\text{N}$  barrier, and a 2-nm UID

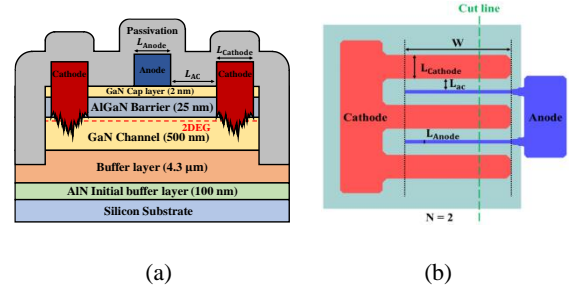


Fig. 1 (a) Schematic cross-section and (b) Layout structure

GaN cap layer, as shown in Fig. 1(a). For the formation of cathode, Ti/Al/Ni/Au Ohmic metal was deposited using thermal evaporation system followed by rapid thermal annealing at 850 °C for 30 seconds in  $\text{N}_2$  ambient, which results in low contact resistance [5].

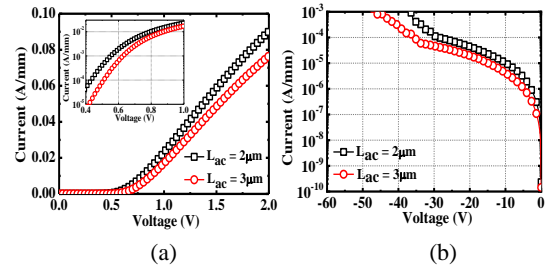


Fig. 2  $I$ - $V$  characteristic  $L_{\text{Anode}}=0.2 \mu\text{m}$ ,  $L_{\text{AC}}=2, 3 \mu\text{m}$ .

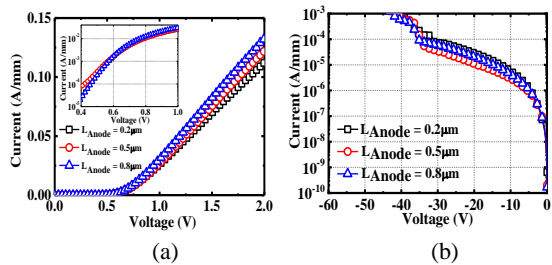


Fig. 3  $I$ - $V$  characteristic  $L_{\text{AC}}=2 \mu\text{m}$ ,  $L_{\text{Anode}}=0.2, 0.5, 0.8 \mu\text{m}$

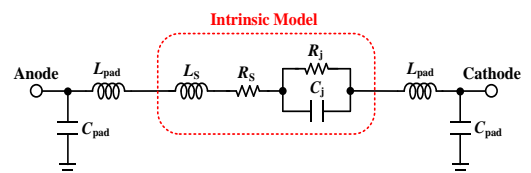


Fig. 4. Small-signal model for AlGaN/GaN SBDs on silicon.

The anode with Ti/Au stack layers was then developed by e-beam lithography to improve the RF performance. It should be mentioned that Ti is used as the Schottky metal instead of the typically used Ni [6]. The lower work function allows a reduced  $V_{on}$ , while  $V_{BK}$  may be degraded. Therefore, different layout geometries are designed to investigate the tradeoff and find out the optimal solution. Finally, device passivation with multilayer structure of  $\text{SiN}_x/\text{SiO}_2/\text{SiN}_x$  was deposited by PECVD system at 300 °C. Note that the finger type layout is adopted, which can be defined by  $W$  (finger width),  $L_{Anode}$  (finger length of anode),  $L_{Cathode}$  (finger length of cathode),  $L_{AC}$  (distance between anode and cathode), and  $N$  (anode finger number). Fig. 1(b) shows the layout of the device with  $N = 2$ . A contact resistance  $R_C$  of 0.5  $\Omega\text{-mm}$  and a sheet resistance  $R_{sh}$  of 413  $\Omega/\square$  were obtained respectively by the Transmission Line Method (TLM) after passivation.

### 3. Results and Discussion

Fig. 2(a) shows the measured results of a two-finger SBD ( $W = 12.5 \mu\text{m}$  and  $L_{Cathode} = 6 \mu\text{m}$ ) with two different  $L_{AC}$  of 2 and 3  $\mu\text{m}$ . A forward current density of 90 mA/mm for  $L_{AC} = 2 \mu\text{m}$  can be achieved. Also,  $V_{on}$  of 0.56 and 0.63 V,  $V_{BK}$  of 37 and 47 V are obtained for the devices with  $L_{AC}$  of 2 and 3  $\mu\text{m}$  respectively, as shown in Fig. 2(b). It was found that tradeoffs exist among forward current,  $V_{on}$  and  $V_{BK}$  regarding the anode-cathode distance. As  $L_{AC}$  reduces, the parasitic access resistance becomes smaller, resulting in improvement of  $V_{on}$  and  $I_D$ . However,  $V_{BK}$  is also degraded due to the smaller distance between the two electrodes. Fig. 3 presents the dependence of device  $V_{on}$  and  $V_{BK}$  on the finger length  $L_{Anode}$ . As can be seen,  $V_{on}$  is not very sensitive to  $L_{Anode}$ , while the current density increases with the finger length (Fig. 3(a)). The increased current density can be attributed to the reduced parasitic anode resistance with an increased  $L_{Anode}$ . A highest current density of 130 mA/mm can be obtained for  $L_{Anode} = 0.8 \mu\text{m}$ . On the other hand, the impact of  $L_{Anode}$  is also not obvious on  $V_{BK}$ , as shown in Fig. 3(b).

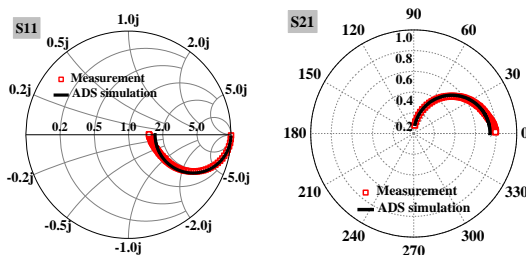


Fig. 5 S-parameter from 100 MHz to 50 GHz with a 100-MHz step.

Fig. 4 shows the small-signal equivalent circuit model including the parasitics for probing pads, where  $C_j$ ,  $R_j$  represent the junction capacitance and resistance, and  $R_s$  and  $L_s$  are the parasitic series resistance and inductance. A good agreement between measured and simulated S-parameters of the intrinsic SBD can be obtained as shown in Fig. 5 ( $L_{AC} = 2 \mu\text{m}$ ,  $L_{Anode} = 0.2 \mu\text{m}$ ). Note that S-parameter measurements

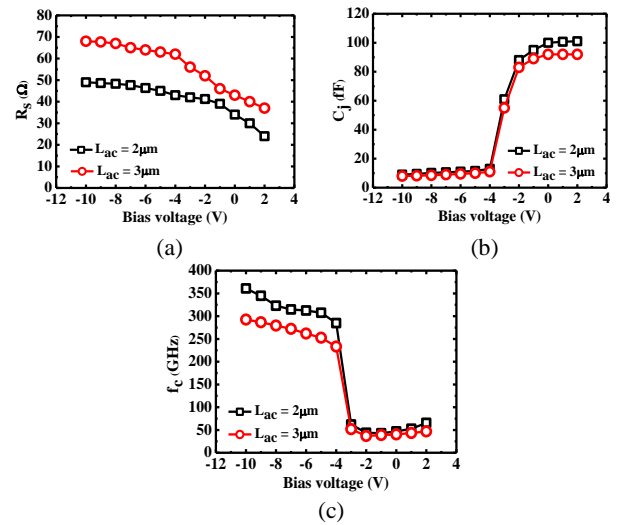


Fig. 6 Extracted values of (a)  $R_s$ , (b)  $C_j$  and (c)  $f_c$ .

at different bias voltages are applied, from where the value of the model parameters can be extracted.

Fig. 6 shows the bias dependence of the key model parameters. As expected,  $R_s$  increases when the bias voltage becomes more negative due to the expansion of the depletion region. As bias voltage exceeds -4 V,  $C_j$  increases rapidly which can also be attributed to the change of depletion region in 2DEG channel. As is shown in Fig. 6(c), when the bias voltage is lower than -4 V, due to the extremely low value of  $C_j$ , the device has increased  $f_c$ . The highest value of  $f_c$  appears at the bias voltage of -10 V for the device with  $L_{AC} = 2 \mu\text{m}$ ,  $L_{Anode} = 0.8 \mu\text{m}$ , which is about 360.9 GHz.

### 4. Conclusions

Aiming for RF energy harvesting applications, GaN Schottky barrier diodes with low turn-on voltage and high breakdown voltage were designed and fabricated in this work. A low  $V_{on}$  and a high  $V_{BK}$  of 0.56 V and 47 V respectively were demonstrated. A high cut-off frequency of 360.9 GHz was also obtained for a two-finger device with each finger of  $W = 12.5 \mu\text{m}$  and  $L = 0.2 \mu\text{m}$ . The analysis based on the extracted small-signal model also provides more insight for the obtained results.

### References

- [1] Song, Y. Huang, J. Zhou, J. Zhang, S. Yuan and P. Carter, *IEEE Transactions on Antennas and Propagation* **63** [8] (2015) 3486.
- [2] Y. Lian, Y. Lin, J. Yang, C. Cheng and S. S. H. Hsu, *IEEE Electron Device Letters* **34** [8] (2013) 981.
- [3] A. Ubukata, K. Ikenaga, N. Akutsu, A. Yamaguchi, K. Matsumoto, T. Yamazaki and T. Egawa, *Journal of Crystal Growth* **298** (2007) 198.
- [4] S. Sugahara, J.S. Lee, K. Ohtsuka, *Jpn. J. Appl. Phys.* **43** (2004), p. L1595
- [5] A. Motayed, R. Bathe, M. C. Wood, O. S. Diouf, R. D. Vispute and S. N. Mohammad, *J. Appl. Phys.* **93** [2] (2003) 1087.
- [6] C.-W. Tsou, K.-P. Wei, Y.-W. Lian and S. S. H. Hsu, *IEEE Electron Device Letters* **37** [1] (2016) 70.